Medical Research | Published by Faculty of Medicine University of Belgrade

ORIGINAL ARTICLE

Anatomical variability and pneumatization patterns of the sphenoid sinus: radiologic analysis

Igor Djoric[1,2,3], Djurdjina Kablar[3,4], Ivan Milic[2,3], Marina Milic[2,3], Lazar Stankovic[2,3], Zoran Radojicic[5], Ana Starcevic[6]

[1]University Clinical Center of Serbia, Center for Radiology Imaging, Belgrade, Serbia
[2]University Clinical Center of Serbia, Clinic of Neurosurgery, Belgrade, Serbia
[3]University of Belgrade, Faculty of Medicine, Belgrade, Serbia
[4]University Clinical Centre of Serbia, Department for Pathology, Pathohistology, and Medical Cytology, Belgrade, Serbia
[5]University of Belgrade, Faculty of Organizational Sciences, Belgrade, Serbia
[6]University of Belgrade, Faculty of Medicine, Institute of Anatomy, Belgrade, Serbia

Submitted: 12 February 2026
Revised: 07 April 2026
Accepted: 09 April 2026
Online First: 15 April 2026

Check for updates

Correspondence to:
Igor Djoric
University Clinical Center of Serbia, Center for Radiology Imaging
2 Pasterova Street, 11000 Belgrade, Serbia
Email: igidren@gmail.com

Summary

Background: Multidetector computed tomography of the sphenoid sinus is the most accurate method for visualizing sinus pneumatization and all anatomical variations.

Objective: To characterize the patterns of pneumatization of the sphenoid sinus and assess the association with variations in the bony structures of the sinus in relation to gender and age groups.

Methods: Retrospective CT analysis of 127 patients (43 men and 84 women). Pneumatization patterns, skull base extensions, and Vidian canal types were classified.

Results: Bilateral increased sphenoid sinus pneumatization shows a very strong age association ($p = 0.001$), with clustering in middle-aged (40–52) and elderly (≥ 66) groups. Right-sided preserved sphenoid sinus pneumatization shows a statistically significant association with gender ($\chi^2 = 3.90$, $p = 0.048$), with a higher proportion of males than females. Bilateral pneumatization (BPP) showed a statistically significant association with age ($p = 0.019$); individuals with BPP were significantly younger. Sellar type predominated (67.7%), with frequent posterior and lateral extensions. The dorsal sphenoid sinus configuration is the only variant showing a statistically significant association with age ($\chi^2 = 8.17$, $p = 0.043$). Complete sellar type shows a strong, consistent positive association with both anterior clinoid and pterygoid process pneumatization on all sides ($p \leq 0.015$, often < 0.001). Type III Vidian canal occurred in ~ 40%. Vidian canal Type I is strongly associated with pterygoid process pneumatization, especially bilaterally ($p < 0.001$ in all cases).

Conclusions: The cohort exhibits a highly pneumatized, surgically relevant sphenoid sinus phenotype, primarily developmental rather than symptom-driven.

Keywords: sphenoid sinus pneumatization, Vidian canal, anterior clinoid process, pterygoid process, multidetector computed tomography.

Cite this article as: Djoric I, Kablar Dj, Milic I, Milic M, Stankovic L, Radojicic Z, Starcevic A.Anatomical variability and pneumatization patterns of the sphenoid sinus: radiologic analysis; Medicinska istraživanja 2026; DOI: 10.5937/medi0-64914

INTRODUCTION

The paranasal cavities include paired sinuses: maxillary (MS), sphenoid (SS), ethmoid (ES), and frontal sinus (FS). The sphenoid sinus (SS) is located in the body of the sphenoid bone, below the sella turcica (ST), and consists of two sections separated from each other by a bony septum. The right and left sphenoid sinuses are usually asymmetrical and may exhibit varying degrees of pneumatization. The degree of pneumatization of the sphenoid sinus has direct implications for endoscopic surgery of the skull base. In newborns, the sphenoid sinus is absent. Pneumatization begins at age 3. At age 7, the pneumatization extends to the sella turcica. At the age of 18, the development is completed (1).

In adults, there are 4 types (variations) of SS pneumatization:

1. conchal (sinus is missing or there is minimal pneumatization)
2. presellar (the most posterior border of the sphenoid sinus is located in front of the anterior wall of the sella turcica)
3. sellar (the sphenoid sinus is located between the anterior and posterior walls of the sella turcica) and
4. postsellar type (the posterior sinus wall exceeds the posterior wall of the sella turcica) (Figure 1) (2).

There are also 4 types of SS extensions:

1. subdorsal (SS pneumatization not crossing the limits of the sellar floor and the Vidian canal)

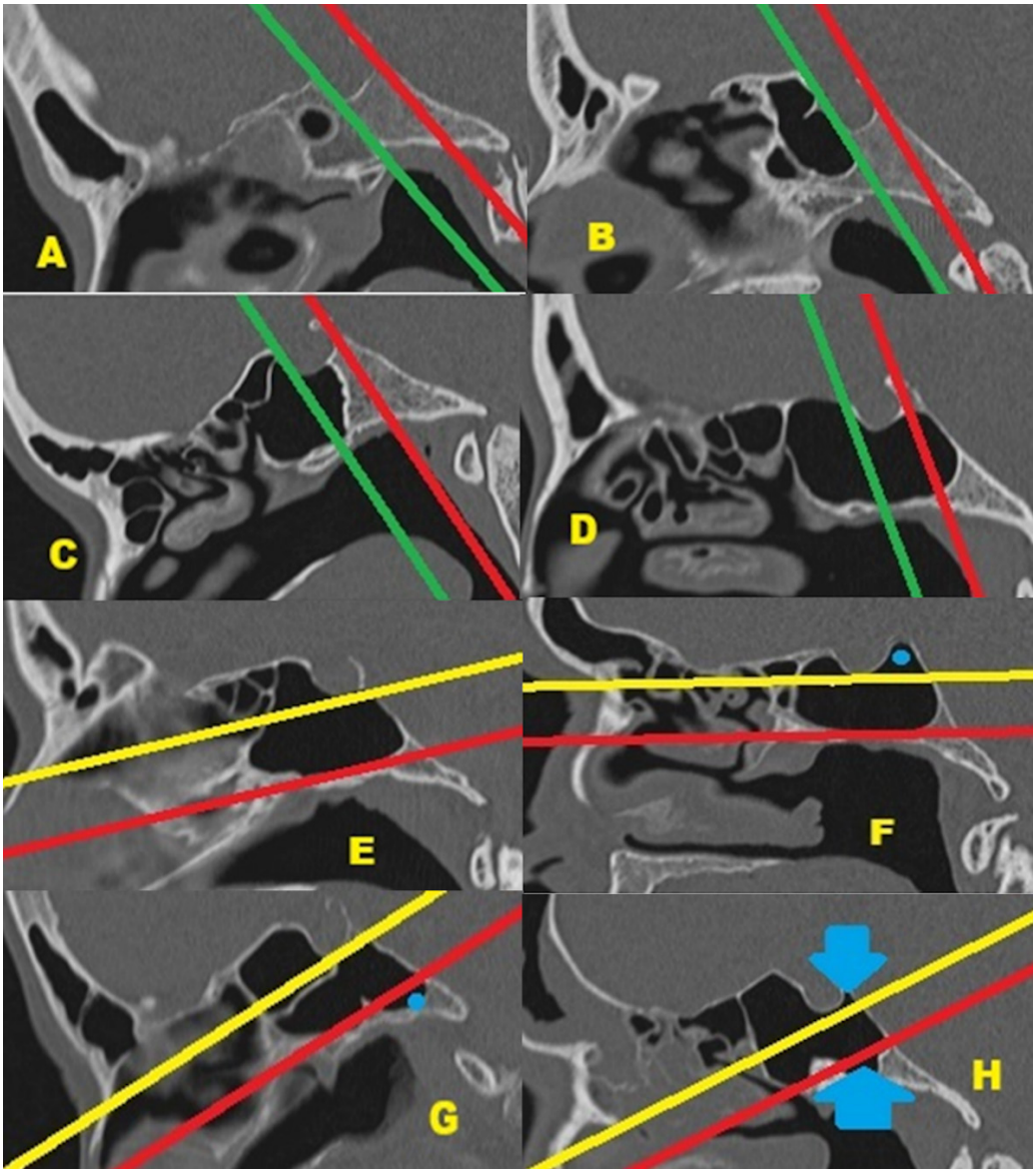

Figure 1. Various types of sphenoid sinus pneumatization and clival extension (MDCT sagittal scan). A – Conchal Type (male, 62 years-old), B – Pressellar Type (female, 44 years-old), C – Incomplete sellar Type (female, 20 years-old), and D – Complete sellar Type (female, 37 years-old). Green line: the anterior wall of the sella, A-D = Red line: the posterior wall of the sella, E - Subdorsal (female, 49 years old), F - Dorsal (male, 66 years old), G - Occipital (female, 74 years old), and H - Combined (Dorsal + Occipital) (male, 45 years old). E-H = Yellow line: the floor of the sella, Red line: limits of Vidian canal, Blue circles and arrowheads: pointing to the extension of the pneumatization. (Illustrative MDCT image selected from the authors' institutional anonymized teaching archive, used solely to demonstrate anatomical classification patterns)

2. dorsal (SS pneumatization extending superiorly into the dorsum sella)
3. occipital (pneumatization extending inferiorly beyond the limits of the Vidian canal)
4. combined (Dorsal + Occipital) **(Figure 1)** (3).

The pterygoid canal (Vidian's canal, VC) is an opening at the base of the skull, located in the pterygoid process of the sphenoid bone, above the pterygoid plates. Vidian's artery and Vidian's nerve pass through it from the middle cranial fossa to the pterygopalatinal fossa (4). The Vidian nerve, formed by the joining of presynaptic parasympathetic fibers and postsynaptic sympathetic fibers, innervates the lacrimal gland, the palate, and the nasal mucosa (5). Three types of Vidian canal are best shown in the coronal projection of multidetector computed tomography (MDCT coronal scan):

1. Type I - canal completely lies within the sinus cavity
2. Type II - canal partially projects into the sinus cavity
3. Type III - canal is surrounded by bone (Figure 2) (6).

The anterior clinoid process (ACP) is a pyramid-shaped bony projection of the lesser wing of the sphenoid bone and forms part of the lateral wall of the optic canal. Between each ACP lies the sella turcica, which holds the pituitary gland. Additionally, the ACP is part of the anterior roof of the cavernous sinus (7). ACP can be aneurysmal or pneumatic, unilateral or bilateral, as best shown in the coronary projection of a multidetector computed tomography (MDCT) coronal scan **(Figure 2)**.

The pterygoid processes or pterygoid plates (PP) are paired postero-inferior protrusions of the sphenoid bone. PP pneumatization often changes the VC's position (8). Both PP and ACP can be aneumatized or pneumaticized unilaterally or bilaterally **(Figure 2)**.

MATERIALS AND METHODS

This retrospective study was conducted in March 2025 at the Department of Neurology of the University Clinical Center of Serbia. All patients underwent MDCT (multidetector computed tomography) of the head and paranasal cavities. The examination was performed according to the standard MDCT protocol for the head at 0.625 mm in the supine position, with the arms lowered to the sides. The field of interest included the regions of the head, paranasal cavities, nasal cavity, and epipharynx. In this way, radiological evaluation of anatomical variations of the sphenoidal sinus was enabled.

Informed consent

All procedures performed in this study involving human participants were conducted in accordance with the ethical standards of the institutional research committee and

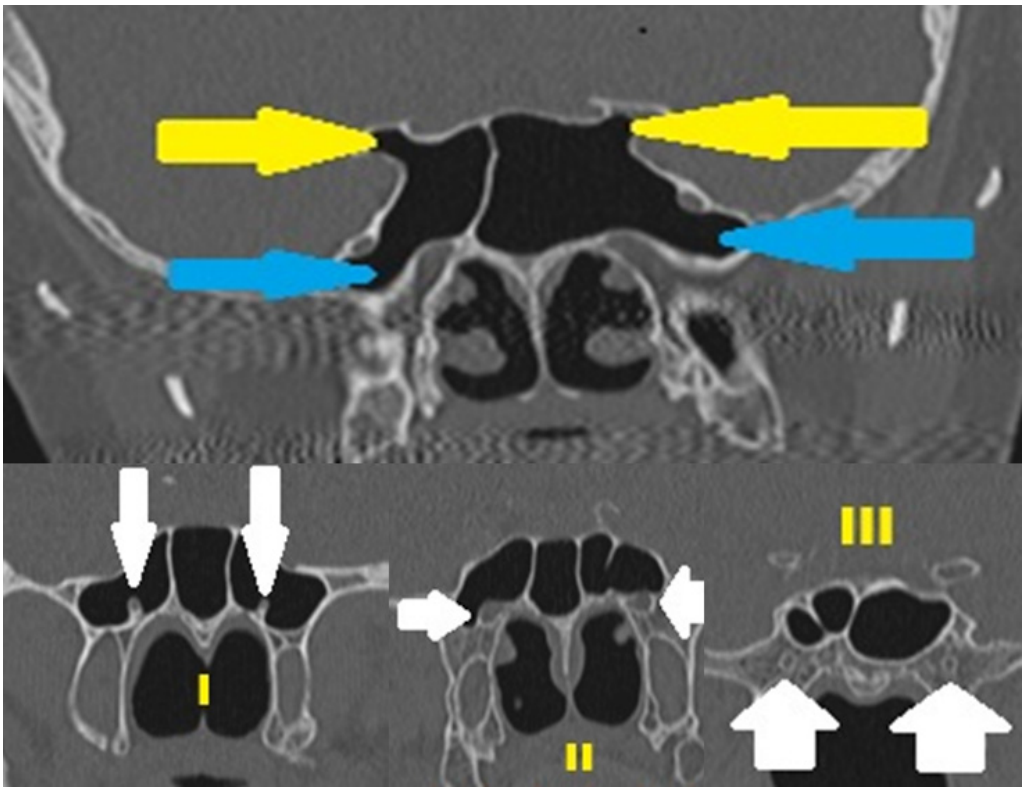

Figure 2. The pneumatization degrees of the sphenoid sinus in the coronal plane are as follows: pterygoid process pneumatization (blue arrows) and anterior clinoid process pneumatization (yellow arrows) and Types of Vidian canal (VC) as assessed on coronal reformatted MDCT images in bone window: I - Bilateral Type I VC (female, 49 years-old), II – Bilateral Type II VC (female, 76 years-old), and III – Bilateral Type III VC (female, 87 years-old). White arrowheads: pointing Vidian canales. (Illustrative MDCT images selected from the authors' institutional teaching archive of anonymized radiological examinations, used solely to demonstrate anatomical classification patterns)

with the principles of the Declaration of Helsinki. This study is a retrospective analysis of multidetector computed tomography (MDCT) examinations originally performed for routine clinical diagnostic purposes. No additional imaging, interventions, or procedures were performed for research purposes. All patient data were anonymized before analysis to ensure confidentiality and privacy. The study protocol was reviewed and approved by the Ethics Committee of the University Clinical Center of Serbia at its 42nd regular session held on February 26, 2026, and the request for written informed consent was waived due to the study's retrospective design and the use of de-identified data.

Subjects

A total of 127 patients (43 men, 84 women) were examined. The patients' ages ranged from 63.4 ± 17.4 years. Represent an older adult population, which is important because sphenoid sinus pneumatization and skull base extensions are developmentally determined but radiologically more visible in older bones.

Patients included in the study were selected by random sampling. These were patients who were referred for MDCT examination of the head according to the following indications: headache, neck pain (cervialgia), dizziness, unsteadiness when walking, tingling, burning and burning of the skin (parestesio cutis), ptosis of the eyelid, loss of consciousness, agitated speech (dysarthria), tremor of the head, tremor of the hands and forgetfulness. Also, patients who have already been diagnosed with neurological diseases - Parkinson's disease, multiple sclerosis, and epilepsy, or associated other diseases - arterial hypertension, diabetes mellitus, and hyperlipidemia - are referred for MDCT examination of the head. None of the patients had endocrinological diseases, pituitary tumors, brain tumors, sinonasal tumors, sinonasal polyposis, cerebrospinal fluid leakage, traumatic lesions of the region of interest, or pronounced facial deformities.

In our retrospective cross-sectional study, the radiological parameters obtained by multidetector computed tomography (MDCT) were related to the pneumatization of the sphenoidal sinus according to the established radiological classifications of the skull base :

1. Sellar Pneumatization Type (Conchal, Presellar, Incomplete sellar, Complete sellar)
2. Directional Pneumatization (Preserved, Reduced, Increased (hyperpneumatization) (assessed separately for right, left, and bilateral sphenoid sinus sections).
3. Posterior Extension (Subdorsal, Dorsal, Occipital, Combined)
4. Lateral Extension: Pterygoid process pneumatization (right/left/bilateral)
5. Vidian Canal Classification (Typ I, II, and III)
6. Anterior Clinoid Process (ACP) Pneumatization : Present/Absent (right/left/bilateral)

Technical considerations of Multidetector Computerized Tomography (MDCT)

Radiologic evaluation via CT was performed with a 256-slice CT (MDCT; Brilliance 6000 iCT solution 256 slice, Philips Medical Systems, Best, The Netherlands) using the following parameters: 0.625 mm section width, 0.625 mm detector width, and 0.4 mm reconstruction interval. Images were sent to a workstation for 0.625 mm reconstruction in axial, coronal, and sagittal planes using bone algorithms.

Statistical analyses

Statistical analysis comprised descriptive and inferential procedures and was performed using IBM SPSS Statistics (version 27.0). Continuous variables were summarized as mean ± standard deviation, while categorical variables were reported as frequencies and percentages. Associations between categorical variables were evaluated using the chi-square test or Fisher's exact test, as appropriate. The interrelationships among binary variables were further explored using a phi coefficient correlation matrix. The results of the phi correlation matrix were visualized using a correlation heatmap to facilitate interpretation of the relationships among anatomical variants. To control for multiple testing, p-values were adjusted using the Benjamini–Hochberg false discovery rate procedure. Predictive modeling of hyperpneumatization was performed using logistic regression analysis. Age, sex, and selected clinical variables were included as predictors, and regression coefficients, odds ratios, and 95% confidence intervals were reported. All analyses examined effects by age, sex, and laterality, and a two-sided p-value < 0.05 was considered statistically significant.

RESULTS

Age of the respondent

Out of a total of 127 examined respondents, the largest number was in the age group of 66 years and over (72 or 56.69%), followed by those in the age group of 53-65 years (22 or 17.32%), then those in the group of 40-52 years (20 or 15.75%) and in the group younger than 40 years (13 or 10.24%) **(Graph 1)**. The patients' ages ranged from 63.4 ± 17.4 years.

Gender of respondents

Of 127 respondents, 84 (66%) were female, and 43 (34%) were male, resulting in a ratio of almost 2:1 in favor of females.

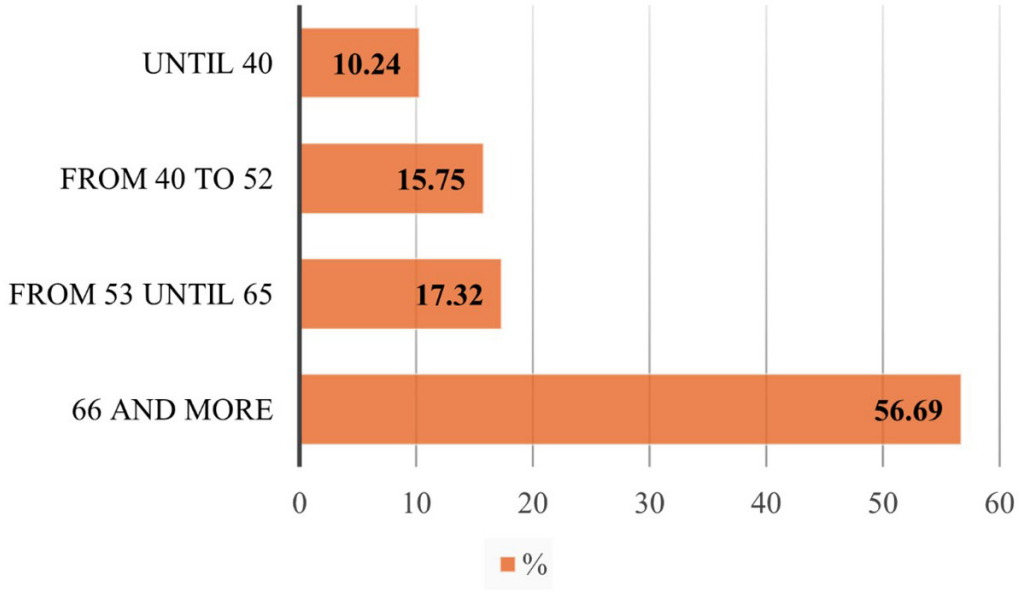

Graph 1. Distribution of patients by age groups

MDCT findings – sphenoid sinus pneumatization (PSS)

MDCT examination of the sphenoid sinus included examination by multiple reconstruction (MPR) in 3 planes – coronal, axial, and sagittal. The degree of pneumatization is classified into three categories: preserved, reduced, or increased pneumatization specifically for the right (PRSS) and left (PLSS) sections and for both sections (PBSS) of the sphenoidal sinus. The degree of SS pneumatization was compared by age group (less than 40 years, 40 to 52 years, 53 to 65 years, and 66 years and older). The test results are shown in **Table 1**.

Preserved sphenoid sinus pneumatization (right, left, bilateral) shows no statistically significant association with age, indicating structural stability across the lifespan. Reduced pneumatization demonstrates a numerical predominance in older subjects (≥ 66 years), particularly on the right side, but does not reach statistical significance, suggesting an age-related tendency without a definitive association. Increased pneumatization exhibits a clear age dependency:

- Right-sided increased pneumatization is significantly associated with age ($p = 0.016$).
- Bilateral increased pneumatization shows a very strong age association ($p = 0.001$), with clustering in the middle-aged (40–52) and elderly (≥ 66) groups.

These findings indicate that excessive or progressive pneumatization, especially when bilateral, is not a random anatomical variant but is significantly influenced by age.

Also, the degree of SS pneumatization was compared by sex, especially for PRSS, PLSS, and PBSS.

Right-sided preserved sphenoid sinus pneumatization shows a statistically significant association with gender ($\chi^2 = 3.90$, $p = 0.048$), with a higher proportion of males than females. All other pneumatization patterns (left-sided, bilateral, reduced, and increased) do not show significant gender differences ($p > 0.05$). Although female predominance is numerically observed across several categories of reduced and increased pneumatization, these differences do not reach statistical significance. They are likely due to the cohort's overall gender distribution. Overall, gender has a limited influence on sphenoid sinus

Table 1. Distribution of sphenoid sinus pneumatization patterns according to age groups (N = 127)

Pneumatization Pattern	Side	≤40 years n (%)	40–52 years n (%)	53–65 years n (%)	≥66 years n (%)	Total n (%)	p-value
Preserved	Right	4 (8.5)	7 (14.9)	11 (23.4)	25 (53.2)	47 (100)	0.571
	Left	5 (11.6)	5 (11.6)	7 (16.3)	26 (60.5)	43 (100)	0.795
	Bilateral	2 (8.3)	3 (12.5)	4 (16.7)	15 (62.5)	24 (100)	0.922
Reduced	Right	2 (5.6)	2 (5.6)	8 (22.2)	24 (66.7)	36 (100)	0.113
	Left	3 (9.4)	2 (6.3)	5 (15.6)	22 (68.8)	32 (100)	0.302
	Bilateral	0 (0.0)	1 (9.1)	2 (18.2)	8 (72.7)	11 (100)	0.547
Increased	Right	7 (15.9)	11 (25.0)	3 (6.8)	23 (52.3)	44 (100)	0.016
	Left	5 (9.6)	13 (25.0)	10 (19.2)	24 (46.2)	52 (100)	0.081
	Bilateral	4 (16.0)	10 (40.0)	1 (4.0)	10 (40.0)	25 (100)	0.001

segment pneumatization, except for the preservation of right-sided pneumatization, which may represent a subtle sex-linked anatomical variation.

MDCT findings – presence of retention content in the sphenoid sinus (RCSS)

Retention (in all cases, inflammatory) content was observed in 13 subjects (10.24%) in the right SS segment, 12 (9.45%) in the left SS segment, and 3 (2.36%) in both SS segments.

All three findings show low prevalence, indicating that retention or loss phenomena in the sphenoid sinus region are uncommon events in the studied population. These findings suggest that retention and destructive changes do not represent major contributors to sphenoid sinus morphology in the examined population.

MDCT findings – pneumatization of pterygoid processes (PPP)

Pneumatization of pterygoid processes (PPP) was determined in the axial and coronal planes by MDCT. Results are especially true for the right (RPP), left (LPP), and both pterygoid processes (BPP). Also, the degree of pneumatization of PPP was compared by age and sex.

Right-sided pneumatization (RPP): Subjects with right pterygoid process pneumatization tended to be younger than those without, as indicated by lower mean ranks; however, this difference did not reach statistical significance ($p = 0.099$), suggesting only a trend toward an age association. Left-sided pneumatization (LPP): age distributions between the pneumatized and non-pneumatized groups were highly overlapping; no statistically significant association between age and left-sided pneumatization was observed ($p = 0.407$). Bilateral pneumatization (BPP): a statistically significant association with age was detected ($p = 0.019$); individuals with bilateral pneumatization were significantly younger, as reflected in substantially lower mean age ranks than in non-bilateral cases; this suggests that bilateral pterygoid process pneumatization is age-dependent, being more prevalent in younger individuals.

Age is not significantly associated with unilateral pterygoid process pneumatization on either the right or left side. In contrast, bilateral pneumatization shows a significant inverse relationship with age, indicating that bilateral involvement is more common in younger subjects. This finding supports the hypothesis that bilateral pneumatization represents a distinct anatomical pattern with potential developmental or age-related determinants.

Right-sided pneumatization (RPP): although females were numerically more represented among the pneumatized cases, the difference between genders was not statistically significant ($\chi^2 = 1.028$, $p = 0.311$). Left-sided pneumatization (LPP): gender distribution was highly similar between the pneumatized and non-pneumatized groups; no gender-related differences were observed ($p = 0.695$). Bilateral pneumatization (BPP): a higher proportion of females was observed in the BPP group; however, this did not reach statistical significance ($p = 0.127$). This finding suggests a non-significant trend, insufficient to support a true gender effect.

Gender is not significantly associated with unilateral or bilateral pterygoid process pneumatization. Despite a consistent numerical predominance of females among pneumatized cases, chi-square and exact tests demonstrate that these differences are compatible with random variation rather than a true sex-related anatomical predisposition.

MDCT findings - sellar pneumatization type and posterior extension of the sphenoid sinus

A sagittal reconstruction of all CT scans was generated, then classified according to sphenoid sinus pneumatization and clival extension (Figure 1). The various types of sphenoid sinus pneumatization: conchal type, presellar type, incomplete sellar type, and complete sellar type **(Graph 2)**. The various types of clival extension: subdorsal, dorsal, occipital, and combined (dorsal + occipital) **(Graph 3)**.

In our study, we examined the correlations between age (by age groups) and sex of respondents, and the types of sphenoid sinus configuration and posterior extension of the sphenoid sinus.

The dorsal sphenoid sinus configuration is the only variant showing a statistically significant association with age ($\chi^2 = 8.17$, $p = 0.043$). This pattern is relatively more frequent in younger and middle-aged groups and less common in older individuals, suggesting a non-random age distribution. All other sphenoid sinus and sellar configuration types show no significant association with age groups ($p > 0.05$), indicating that their prevalence largely reflects the cohort's underlying age structure. Although many variants (conchal, incomplete sellar, complete sellar, subdorsal, occipital) appear numerically more frequent in the ≥ 66 years group, this mirrors the overall population distribution and does not represent a true age-dependent effect. Overall, sphenoid sinus pneumatization and sellar configuration types are predominantly age-independent anatomical variants, with the notable exception of the dorsal sphenoid sinus pattern.

No sphenoid sinus or sellar configuration type showed a statistically significant association with gender ($p > 0.05$ for all comparisons). Although female predominance was numerically observed in several variants (conchal, incomplete sellar, combined SS), these differences did not exceed random variation, as confirmed by chi-square and Fisher's exact testing. More complex anatomical variants (dorsal, occipital, combined SS) also demonstrated gender-neutral distributions, indicating

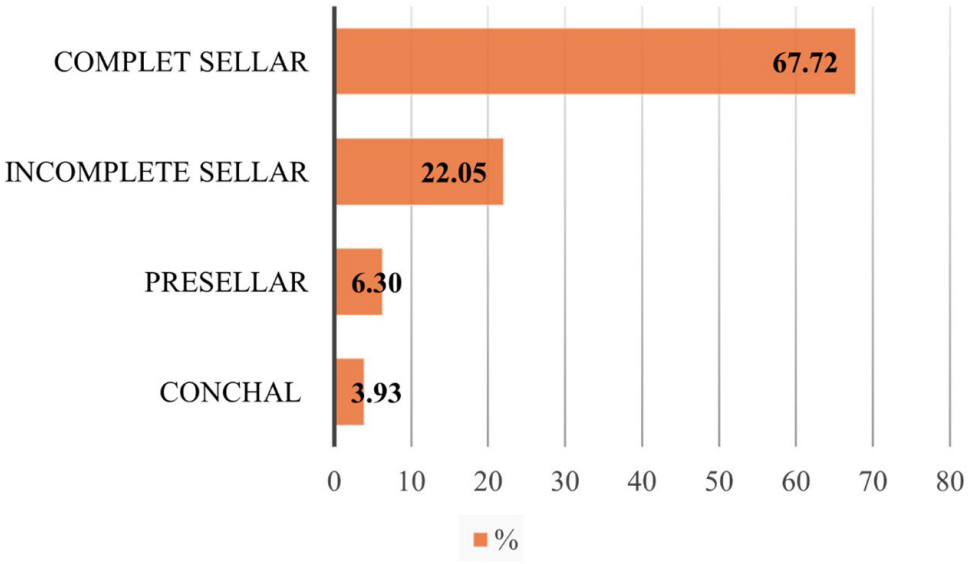

Graph 2. Types of sphenoid sinus pneumatization

that these morphologic patterns are not sex-dependent. The findings support the interpretation that pneumatization pattern and sellar/sphenoid sinus morphology are developmentally determined anatomical variants, largely independent of sex.

MDCT findings – correlation of types of pneumatization of the sphenoid sinus and its posterior extension with pneumatization of anterior clinoid processes (ACP) and pneumatization of pterygoid processes (PP)

The analysis of the relationship between the types of sphenoid sinus pneumatization and its posterior extension with anterior clinoid process pneumatization (ACP) and pterygoid process pneumatization (PP) was interpreted in the coronal MDCT plane. The test results are shown in **Table 2**.

Values are presented as absolute numbers (n) and percentages within each sphenoid sinus type. Associations were tested using Pearson χ^2 or Fisher's exact test, as appropriate.

Sellar configuration is a major determinant of skull-base pneumatization. Complete sellar type shows a strong, consistent positive association with both ACP and pterygoid process pneumatization on all sides ($p \leq 0.015$, often < 0.001). Incomplete sellar and subdorsal configurations act as restrictive patterns. These types are significantly associated with reduced ACP and pterygoid pneumatization, indicating limited aeration of the skull base. Conchal and occipital types are considered neutral anatomical variants, with no statistically significant association with pneumatization patterns. Combined and dorsal sphenoid sinus types represent advanced pneumatization phenotypes, strongly linked—especially bilaterally—to pterygoid process pneumatization. The

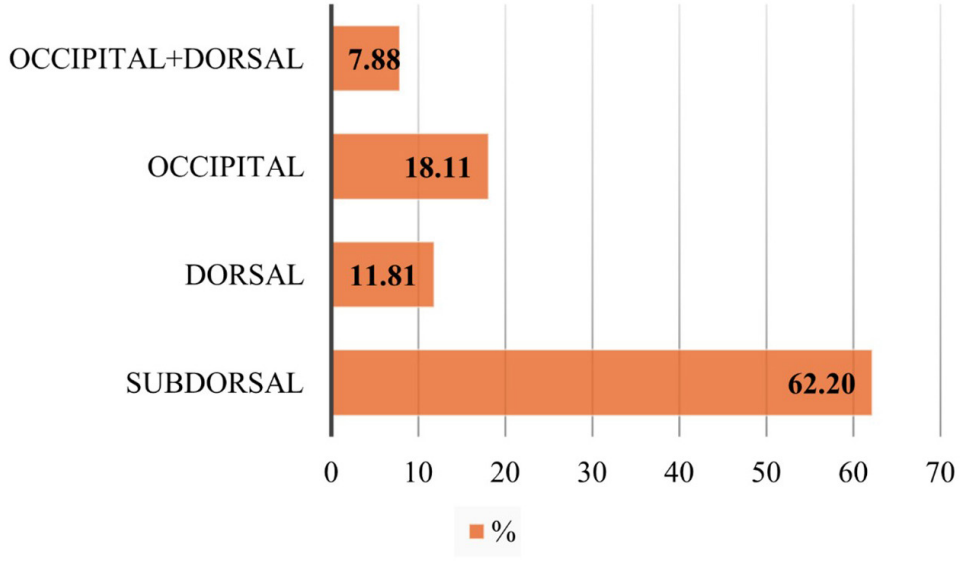

Graph 3. Types of posterior (clival) sphenoid sinus extensions

Table 2. Association between sphenoid sinus pneumatization types and pneumatization of adjacent structures (ACP and pterygoid processes) (N = 127)

Sphenoid Sinus Type	Structure	Side	Pneumatization Present N (%)	Pneumatization Absent N (%)	Total N	p-value
Conchal	ACP	Right	1 (20.0)	4 (80.0)	5	0.832
		Left	0 (0.0)	5 (100)	5	0.339
		Bilateral	0 (0.0)	5 (100)	5	0.482
	Pterygoid process	Right	0 (0.0)	5 (100)	5	0.103
		Left	1 (20.0)	4 (80.0)	5	0.268
		Bilateral	0 (0.0)	5 (100)	5	0.195
Presellar	ACP	Right	0 (0.0)	8 (100)	8	0.193
		Left	0 (0.0)	8 (100)	8	0.220
		Bilateral	0 (0.0)	8 (100)	8	0.368
	Pterygoid process	Right	0 (0.0)	8 (100)	8	0.037
		Left	1 (12.5)	7 (87.5)	8	0.063
		Bilateral	0 (0.0)	8 (100)	8	0.097
Incomplete sellar	ACP	Right	1 (3.6)	27 (96.4)	28	0.036
		Left	0 (0.0)	28 (100)	28	0.012
		Bilateral	0 (0.0)	28 (100)	28	0.065
	Pterygoid process	Right	5 (17.9)	23 (82.1)	28	0.043
		Left	7 (25.0)	21 (75.0)	28	0.021
		Bilateral	4 (14.3)	24 (85.7)	28	0.158
Complete sellar	ACP	Right	19 (22.1)	67 (77.9)	86	0.015
		Left	19 (22.1)	67 (77.9)	86	0.001
		Bilateral	11 (12.8)	75 (87.2)	86	0.017
	Pterygoid process	Right	38 (44.2)	48 (55.8)	86	<0.001
		Left	47 (54.7)	39 (45.3)	86	0.001
		Bilateral	27 (31.4)	59 (68.6)	86	0.008
Subdorsal	ACP	Right	8 (10.1)	71 (89.9)	79	0.013
		Left	6 (7.6)	73 (92.4)	79	0.003
		Bilateral	2 (2.5)	77 (97.5)	79	0.002
	Pterygoid process	Right	18 (22.8)	61 (77.2)	79	0.001
		Left	27 (34.2)	52 (65.8)	79	0.004
		Bilateral	13 (16.5)	66 (83.5)	79	0.007
Dorsal	ACP	Right	5 (33.3)	10 (66.7)	15	0.062
		Left	4 (26.7)	11 (73.3)	15	0.176
		Bilateral	4 (26.7)	11 (73.3)	15	0.008
	Pterygoid process	Right	9 (60.0)	6 (40.0)	15	0.023
		Left	9 (60.0)	6 (40.0)	15	0.186
		Bilateral	6 (40.0)	9 (60.0)	15	0.134
Occipital	ACP	Right	5 (21.7)	18 (78.3)	23	0.458
		Left	5 (21.7)	18 (78.3)	23	0.314
		Bilateral	3 (13.0)	20 (87.0)	23	0.409
	Pterygoid process	Right	8 (34.8)	15 (65.2)	23	0.918
		Left	12 (52.2)	12 (52.2)	23	0.388
		Bilateral	5 (21.7)	5 (21.7)	23	0.742

observed associations are directionally coherent and anatomically consistent, supporting a developmental–morphologic continuum rather than random variation.

MDCT findings – distribution of Vidian's canal

The types of Vidian's canal (I, II, and III) were determined in a coronal MDCT projection (coronal MDCT scan).

Type III Vidian canal is the predominant anatomical variant, accounting for the most frequent configuration on both the right and left sides (≈ 40%) and the most common bilateral form (≈ 33%). Types I and II occur at similar frequencies on the right and left sides, demonstrating high lateral symmetry and suggesting stable developmental patterning rather than side dominance. Bilateral occurrence is consistently less frequent than

Table 3. Association between Vidian canal type and pterygoid process pneumatization according to side (N = 127)

Side	Vidian Canal Type	Pneumatization Present N (%)	Pneumatization Absent N (%)	Total N (%)	p-value
Right	Type I	28 (80.0)	7 (20.0)	35 (100)	<0.001
	Type II	12 (30.8)	27 (69.2)	39 (100)	0.624
	Type III	3 (5.9)	48 (94.1)	51 (100)	<0.001
Left	Type I	28 (77.8)	8 (22.2)	36 (100)	<0.001
	Type II	19 (50.0)	19 (50.0)	38 (100)	0.381
	Type III	9 (17.6)	42 (82.4)	51 (100)	<0.001
Bilateral	Type I	23 (74.2)	8 (25.8)	31 (100)	<0.001
	Type II	6 (20.7)	23 (79.3)	29 (100)	0.596
	Type III	1 (2.4)	41 (97.6)	42 (100)	<0.001

unilateral presence for all VC types, indicating that full bilateral symmetry is the exception rather than the rule. The overall distribution shows a clear hierarchical prevalence pattern: Type III > Type II ≈ Type I, both unilaterally and bilaterally.

Vidian canal morphology demonstrates a symmetric and non-random distribution, with Type III representing the dominant anatomical configuration. Types I and II occur at comparable rates and are less frequently expressed bilaterally. This baseline distribution provides essential anatomical context for interpreting the strong associations observed between Vidian canal type and pterygoid process pneumatization.

MDCT findings – association of Vidian canal types with pneumatization of pterygoid processes

The analysis of the association of Vidian canal types with pneumatization of pterygoid processes was determined in a coronal MDCT projection (coronal MDCT scan). The test results are shown in **Table 3**.

Values are presented as absolute numbers (n) and percentages within each Vidian canal type. Associations were tested using the χ^2 test.

Vidian canal Type I is strongly and consistently associated with pterygoid process pneumatization on the right, left, and especially bilaterally ($p < 0.001$ in all cases) → Type I VC is a robust anatomical marker of pneumatized pterygoid processes. Vidian canal Type III shows a strong inverse association with pneumatization across all sides ($p < 0.001$) → Type III VC is predominantly observed in non-pneumatized pterygoid processes. Vidian canal Type II demonstrates no statistically significant association with pneumatization on any side ($p > 0.38$ in all analyses) → Type II VC appears anatomically neutral with respect to pterygoid pneumatization. The bilateral configuration shows the strongest effects, indicating that bilateral pneumatization represents a distinct, highly structured anatomical pattern rather than a random or incidental variant.

Pneumatization of the pterygoid process is not randomly distributed with respect to Vidian canal morphology. Instead, it demonstrates a highly structured anatomical relationship, characterized by a strong association with Vidian canal Type I and a marked exclusion of Type III, particularly in bilateral cases. These findings have important implications for preoperative planning and risk stratification in endoscopic endonasal and skull-base procedures.

Correlation analysis of anatomical variants

To explore interrelationships among binary anatomical variables, a phi coefficient correlation matrix was calculated. The analysis demonstrated structured clustering of pneumatization patterns rather than random distribution.

Strong positive correlations were observed between the complete sellar type and pneumatization of both the anterior clinoid process (ACP) and pterygoid processes, particularly when these structures were bilaterally pneumatized. These correlations support the concept that advanced sellar pneumatization reflects a broader developmental expansion of sphenoid sinus aeration into adjacent skull base structures.

In contrast, incomplete sellar and subdorsal configurations demonstrated negative correlations with ACP and pterygoid pneumatization, indicating restricted aeration patterns.

Lateral recess markers, including pterygoid process pneumatization and Vidian canal variants, also demonstrated moderate correlations with directional sphenoid sinus pneumatization patterns.

Overall, the phi matrix confirmed that sphenoid sinus anatomical variants follow a developmental pneumatization continuum, rather than representing independent random findings. The relationships among major anatomical variants were further explored using a phi coefficient correlation matrix **Graph 4**. The phi coefficient matrix was computed using the 20 most prevalent binary anatomical variables to ensure stable estimation and avoid sparse-cell artifacts. Variables listed in the legend. (legend numbers 1–20)

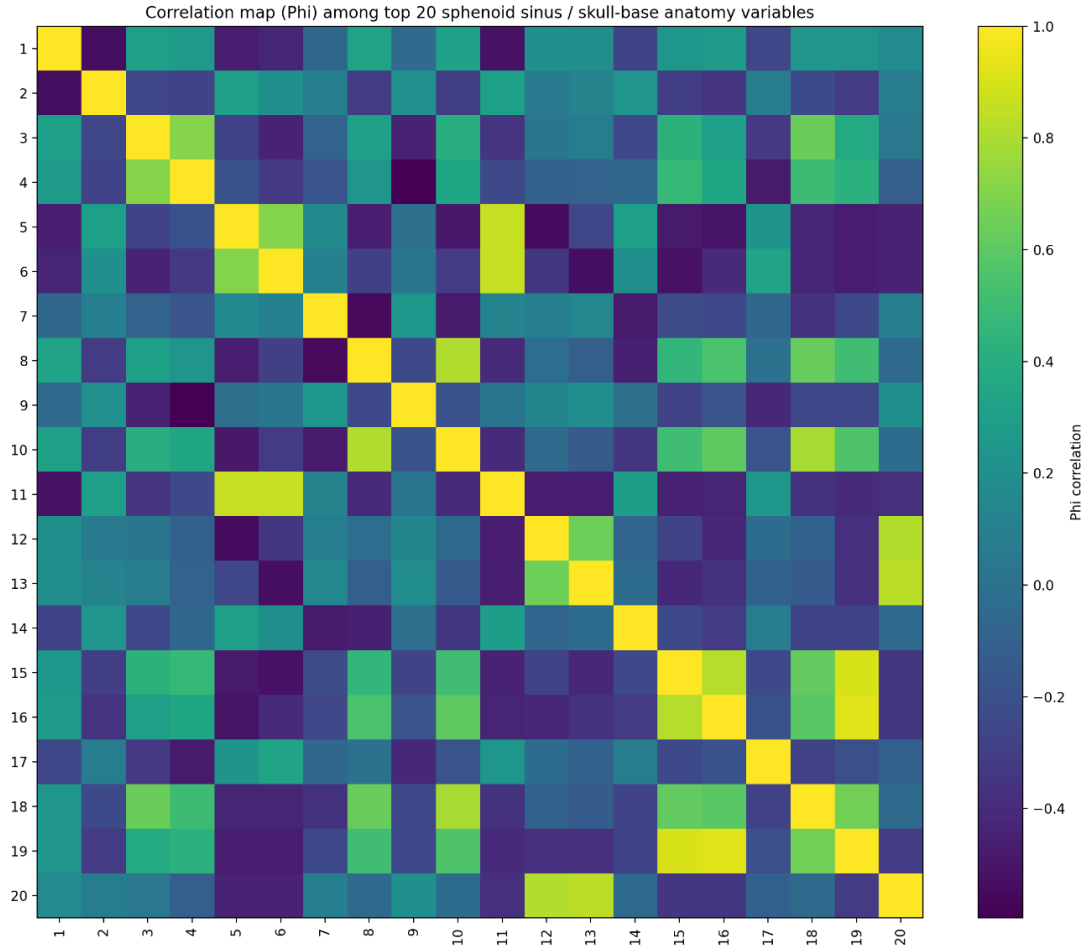

Graph 4. Correlation structure of anatomical variants (Phi coefficient matrix)

(Phi matrix variables (1–20) — top 20 most prevalent anatomy/pneumatization variables n (%)

1. COMPLET SELLAR TYPE PSS — 86 (67.7%)
2. SUBDORSAL SS — 79 (62.2%)
3. PNEUMATISATION PTERYGOID PROCESS SIN. — 56 (44.1%)
4. LEFT SS SEGMENT PNEUMATIZATION INCREASED — 52 (40.9%)
5. TYP III VIDIAN CANAL (VC) DEX. — 51 (40.2%)
6. TYP III VIDIAN CANAL (VC) SIN. — 51 (40.2%)
7. PNEUMATICATION OF THE RIGHT SS SECTION PRESERVED — 47 (37.0%)
8. PNEUMATICIZATION OF THE RIGHT SS SECTION INCREASED — 44 (34.6%)
9. LEFT SECTION SS PNEUMATIZATION PRESERVED — 43 (33.9%)
10. PNEUMATISATION PTERYGOID PROCESS DEX. — 43 (33.9%)
11. TYP III VIDIAN CANAL (VC) BILL. — 42 (33.1%)
12. TYP II VIDIAN CANAL (VC) DEX. — 39 (30.7%)
13. TYP II VIDIAN CANAL (VC) SIN. — 38 (29.9%)
14. PNEUMATICIZATION OF THE RIGHT SS SECTION REDUCED — 36 (28.3%)
15. TYP I VIDIAN CANAL (VC) SIN. — 36 (28.3%)
16. TYP I VIDIAN CANAL (VC) DEX. — 35 (27.6%)
17. LEFT SECTION SS PNEUMATIZATION REDUCED — 32 (25.2%)
18. PNEUMATISATION PTERYGOID PROCESS BILL. — 31 (24.4%)
19. TYP I VIDIAN CANAL (VC) BILL. — 31 (24.4%)
20. TYP II VIDIAN CANAL (VC) BILL. — 29 (22.8%)

Predictors of sphenoid sinus hyperpneumatization

To explore potential predictors of increased sphenoid sinus pneumatization, a logistic regression analysis was performed. Hyperpneumatization (defined as increased pneumatization in at least one sphenoid sinus section) was used as the dependent variable, while age, sex, and selected neurological symptoms were entered as independent variables.

The analysis demonstrated that age showed a modest inverse association with hyperpneumatization, suggesting that younger individuals were more likely to exhibit hyperpneumatization. However, this association did not reach strong statistical significance. Sex and clinical symptoms exerted only minimal predictive influence, suggesting that hyperpneumatization is largely independent of clinical presentation and may primarily reflect developmental anatomical variation. The results of the logistic regression analysis are presented in **Table 4**.

DISCUSSION

The use of multidetector computed tomography (MDCT) remains the gold standard for evaluating the anatomy and pneumatization patterns of the paranasal sinuses, including the sphenoid sinus, due to its high spatial resolution and ability to accurately depict fine bony details. This allows precise assessment of anatomical variations that may have important clinical implications.

The present study aimed to determine the prevalence of sphenoid sinus pneumatization types and posterior (clival) extension patterns, and to examine their relationships with demographic factors and adjacent anatomical structures.

Special emphasis was placed on the correlation between sphenoid sinus pneumatization and the pneumatization of the anterior clinoid processes (ACP) and pterygoid processes (PP), as well as their association with Vidian canal (VC) types.

In this current study, the prevalence of sellar, incomplete sellar, presellar, and conchal types of sphenoid pneumatization was 68%, 22%, 6%, and 4%, respectively **(Graph 2)**. These findings are consistent with the results of a study by Açar and the authors (9). The most prevalent SSSP type was postsellar (62.7%), followed by sellar (30%), presellar (6.6%), and conchal (0.7%). Singh and the authors (10) also show similar results. However, the higher prevalence of postsellar pneumatization reported by Tavakoli et al. (82.5%) compared to our results (62%) may be attributed to differences in sample size, population characteristics, or imaging criteria. This suggests that demographic or methodological factors may influence anatomical variation.

When it comes to the types of posterior (clival) extension of the sphenoid sinus, in our study, the sudorsal type is the most common (62%), followed by the occipital type (18%), the dorsal type (12%), and the combined (occipital + dorsal) type (8%) **(Graph 3)**. These results are similar to those of the previous study (10).

In our study, pneumatization of the right anterior clinoid process was detected in 21 subjects (16.5%), pneumatization of the left anterior clinoid process in 19 (15%), and pneumatization of both anterior clinoid processes in 11 (about 9%). Sagar et al. (12) reported a 26.3% (n=30) prevalence of pneumatization of the anterior clinoid process (ACP). According to sphenoid sinus types, ACP pneumatization was absent in the conchal type, while occurring in 2.6% (n=3) of the presellar type and 23.5% (n=27) of the sellar type. Unilateral pneumatization was observed in 11.4% (n=13) and bilateral in 14.9% (n=17) of cases, with no significant predilection for either the right or left side. Ali et al. (13) reported a 13.3% (n=14) prevalence of anterior clinoid process (ACP) pneumatization. Burulday et al. (14) reported similar findings in their study.

In our study, pneumatization of the right pterygoid process was present in 43 subjects (34%), pneumatization of the left pterygoid process in 56 subjects (44%), and pneumatization of both pterygoid processes in 31 subjects (24%). The observed inverse relationship between age and bilateral pneumatization may reflect developmental patterns of sphenoid sinus expansion, which is known to progress during adolescence and early adulthood. Alternatively, this finding could be influenced by sampling bias and should therefore be interpreted with caution. In a study by Sagar et al. (12), pterygoid process (PP) pneumatization was identified in 23.6% of cases. The distribution across sphenoid types was 0% conchal, 4.4% presellar, and 19.2% sellar. The authors reported bilateral involvement in 14% of subjects and unilateral involvement in 9.6%, noting no significant predilection

Table 4. Logistic regression analysis of predictors of sphenoid sinus hyperpneumatization (Model performance: AUC = 0.58)

Predictor	β coefficient	Odds Ratio (OR)	95% CI	p-value
Age	-0.23	0.79	0.58–1.07	0.12
Male sex	-0.08	0.93	0.53–1.62	0.78
Headache	0.08	1.09	0.59–2.01	0.79
Dizziness	0.04	1.04	0.53–2.04	0.90
Instability when walking	-0.02	0.98	0.53–1.83	0.95
Forgetfulness	0.24	1.28	0.63–2.58	0.49

for either side. In Ali et al. (13), pneumatization of the pterygoid processes was detected bilaterally in 25% of respondents.

Although a statistically significant association was found between the complete sellar type and ACP and pterygoid process pneumatization ($p \leq 0.015$), the cross-sectional design of this study limits the ability to infer causality. Further studies are needed to determine whether this relationship reflects shared developmental pathways or coincidental anatomical variation. In our study, 28 subjects (22%) had type I of the Vidian canal (VC) on the right, 12 (9%) had type II (9%), and 3 (2%) had type III VC. Type I VC on the left accounted for 28 (22%), type II for 19 (15%), and type III for 9 (7%). Type I VC was bilaterally present in 23 subjects (18%), type II VC in 6 (5%), and type III VC in only 1 respondent (0.8%). Mohebbi et al. (15) reported the prevalence of Vidian canal types I, II, and III as 28%, 48%, and 24%, respectively. Our results regarding the distribution of the right-sided Vidian canal are consistent with those reported by Yeğin et al. (16).

CONCLUSIONS

Multidetector computed tomography (MDCT) provides a reliable and detailed evaluation of sphenoid sinus pneumatization and associated anatomical variations, including the anterior clinoid processes, pterygoid processes, and Vidian canal morphology. The present study demonstrates that sellar-type pneumatization and subdorsal posterior extension are the most prevalent anatomical patterns, with significant associations observed between complete sellar pneumatization and adjacent structural pneumatization. These findings contribute to a more comprehensive understanding of sphenoid sinus anatomical variability and suggest potential underlying developmental relationships.

From a clinical standpoint, precise preoperative identification of these variations is essential for reducing the risk of complications during endonasal endoscopic and transsphenoidal surgical procedures. Although MDCT remains a key imaging modality in this setting, its findings should be interpreted in the context of clinical factors and surgical expertise.

Further large-scale, multicenter, and longitudinal studies are warranted to validate these findings and better define their developmental and clinical significance.

Acknowledgments: N/A

Funding information: The authors state that this study has not received any funding.

Conflicts of interest: The authors declare no conflict of interest.

Author contributions: Study conception and design: IDJ, DJK, AS; Data collection: IDJ, IM, MM, LS; Analysis and interpretation of results: IDJ, ZR, AS; Draft manuscript preparation: IDJ, ZR; Critical revision of the article: IDJ, ZR, AS.

All authors reviewed the results and approved the final version of the manuscript.

Ethical approval: Ethics Committee of the University Clinical Center of Serbia – No. 181/1, February 26, 2026.

Informed consent: N/A

REFERENCES

1. Wolf G, Anderhuber W, Kuhn F. Development of the paranasal sinuses in children: implications for paranasal sinus surgery. Ann Otol Rhinol Laryngol. 1993 Sep;102(9):705-11. DOI: 10.1177/000348949310200911. PMID: 8373095.
2. Aijaz A., Ahmed H., Fahmi Sh., Samreen T., Rasheed B, Jabeen H. A Comprehensive Computed Tomographic Analysis of Pneumatization Pattern of Sphenoid Sinus and Their Association with Protrusion/Dehiscence of Vital Neurovascular Structure in a Pakistani Subgroup. Turk Neurosurg 33(3):501-508, 2023. DOI: 0.5137/1019-5149.JTN.40154-22.3
3. Nepal, P. R., Karki, K. T., & Rajbanshi, J. N. Types of Sphenoid Sinus Pneumatization among Nepalese Population. Egneuro, 02(03):14–18, 2020 DOI: 10.3126/egn.v2i3.31468
4. Bidarkotimath S., Viveka S., and Udyavar A. Vidian canal: radiological anatomy and functional correlations. J. Morphol. Sci ., 2012, vol. 29, no. 1, p. 27-31
5. Su WF, Liu SC, Hsu WC, Chen YC. Randomized, double-blind, controlled study to evaluate the effect of vidian nerve cauterization on lacrimation. I'm allergic to Rhinol. 2014; 28 (3):255 –259. DOI: 10.2500/ajra.2014.28.4029 PMID: 24980238
6. Ramanna HC, Gowda SS, Jithendra N, et al. A Radio-Anatomic Profile of the Sphenoid Sinus, Vidian Canal and Foramen Rotundum Structured. J Evid Based Med Healthc 2020; 7 (40), 2294-2299. DOI: 10.18410/jebmh/2020/476
7. da Costa, Marcos Devanir Silva MD, MSc; de Oliveira Santos, Bruno Fernandes MD; de Araujo Paz, Daniel MD; Rodrigues, Thiago Pereira MD; Abdala, Nitamar MD, PhD; Centeno, Ricardo Silva MD, PhD; Cavalheiro, Sergio MD, PhD; Lawton, Michael T. MD; Chaddad-Neto, Feres MD, PhD. Anatomical Variations of the Anterior Clinoid Process: A Study of 597 Skull Base Computerized Tomography Scans. Operative Neurosurgery 12(3): p. 289-297, September 2016. | DOI: 10.1227/NEU.0000000000001138
8. Kaplanoğlu H, Kaplanoğlu V, Dilli A, Toprak U, Hekimoğlu B. An analysis of the anatomic variations of the paranasal sinuses and ethmoid roof using computed tomography. Eurasian J Med. 2013 Jun; 45 (2):115 -25. DOI: 10.5152/eajm.2013.23. PMID: 25610263; PMCID: PMC4261488.
9. Açar, G., Gökşan, A.S. & Aydoğdu, D. Computed tomography-based evaluation of the association between sphenoid sinus pneumatization patterns and variations of adjacent bony structures in relation to age and gender. Neurosurg Rev 47, 349 (2024). DOI: 10.1007/s10143-024-02594-8
10. Singh A, Kameshwarachar M, Singh H. Assessment of Variations in Sphenoid Sinus Pneumatization in South Indian Population. BJOHNS [Internet]. 2022Mar .18 [cited 2026Feb.8]; 29(3):279-84. DOI: 10.47210/bjohns.2021.v29i3.489
11. Tavakoli, M., Jafari-Pozve, N. & Aryanezhad, S. Sphenoid Sinus Pneumatization Types and Correlation with Adjacent Neurovascular Structures Using Cone-Beam Computed Tomography. Indian J

Otolaryngol Head Neck Surg 75, 2245–2250 (2023). DOI: 10.1007/s12070-023-03796-0

12. Sagar, S., Jahan, S. & Kashyap, S.K. Prevalence of anatomical variations of sphenoid sinus and its adjacent structures: Pneumatization and its significance: a CT scan study. Indian J Otolaryngol Head Neck Surg 75, 2979–2989 (2023). DOI: 10.1007/s12070-023-03879-y
13. Akbar Ali, M., Manish Jaiswal, D., Sameer Ahamed, D.B. et al. A Study of Anatomical Variations of Sphenoid Sinus on CT PNS: Our Experience. Indian J Otolaryngol Head Neck Surg 74 (Suppl 2), 1690–1693 (2022). DOI: 10.1007/s12070-021-02842-z
14. Burulday V, Muluk NB, Akgül MH, Kaya A, Öğden M. Presence and types of anterior clinoid process pneumatization, evaluated by Multidetector Computerized Tomography. Clin Invest Med. 2016 Jun 16;39(3):E105-10. DOI: 10.25011/cim.v39i3.26799. PMID: 27439685.
15. Mohebbi A, Rajaeih S, Safdarian M, Omidian P. The sphenoid sinus, foramen rotundum, and vidian canal: a radiological study of anatomical relationships. Braz J Otorhinolaryngol. 2017 Jul-Aug;83(4):381-387. DOI: 10.1016/j.bjorl.2016.04.013. Epub 2016 May 24. PMID: 27283380; PMCID: PMC9442688.
16. Yeğin Y, Çelik M, Altıntaş A, Şimşek BM, Olgun B, Kayhan FT. Vidian Canal Types and Dehiscence of the Bony Roof of the Canal: An Anatomical Study. Turk Arch Otorhinolaryngol. 2017 Mar; 55 (1):22 -26. doi: 10.5152/tao.2017.2038. Epub 2017 March 1. PMID: 29392047; PMCID: PMC5782923.
17. Zengin HH, Öztürk D, Sarı MA, Özdemir S. Evaluation of the Relationship of Sphenoid Sinus Pneumatization with Adjacent Neurovascular Structures Using Computed Tomography. Work & Mol Image 2024; 1(1):5-10. DOI: 10.70087/rami.tui/010104
18. Dogan ME, Kotanlı S, Yavuz Y, Wahjuningrum DA, Pawar AM. 2023. Computed tomography-based assessment of sphenoid sinus and sella turcica pneumatization analysis: a retrospective study. PeerJ 11:e16623 DOI: 10.7717/peerj.16623
19. Alam-Eldeen MH, ElTaher MA, Fadle KN. CT evaluation of pterygoid process pneumatization and the anatomic variations of related neural structures. Egyptian Journal of Radiology and Nuclear Medicine (Online). 2018;49(3):p. 658–662. DOI:10.1016/j.ejrnm.2018.03.011

ANATOMSKA VARIJABILNOST I OBRASCI PNEUMATIZACIJE SFENOIDALNOG SINUSA: RADIOLOŠKA ANALIZA

Igor Đorić[1,2,3], Đurđina Kablar[3,4], Ivan Milić[2,3], Marina Milić[2,3], Lazar Stanković[2,3], Zoran Radojičić[5], Ana Starčević[6]

Sažetak

Uvod: Multidetektorska kompjuterizovana tomografija sfenoidalnog sinusa je najpreciznija metod za vizuelizaciju pneumatizacije sinusa i svih anatomskih varijacija.

Cilj: Karakterizirati obrasce pneumatizacije sfenoidalnog sinusa i proceniti povezanost sa varijacijama u koštanim strukturama sinusa u odnosu na pol i starosne grupe.

Metode: Retrospektivna CT analiza 127 pacijenata (43 muškarca i 84 žene). Obrasci pneumatizacije, proširenja baze lobanje i tipovi Vidian kanala su klasifikovani.

Rezultati: Bilateralna povećana pneumatizacija sfenoidalnog sinusa pokazuje veoma jaku starosnu asocijaciju (p = 0,001), sa grupiranjem u sredovečnim (40–52) i starijim (≥ 66) grupama. Očuvana pneumatizacija sfenoidalnog sinusa desno pokazuje statistički značajnu povezanost sa polom (χ^2 = 3,90, p = 0,048), sa većim udelom muškaraca nego žena. Bilateralna pneumatizacija (BPP): otkrivena je statistički značajna povezanost sa godinama (p = 0,019); pojedinci sa BPP su bili znatno mlađi. Preovlađuje sellarni tip (67,7%), sa čestim zadnjim i bočnim ekstenzijama. Konfiguracija dorzalnog sfenoidalnog sinusa je jedina varijanta koja pokazuje statistički značajnu povezanost sa godinama (χ^2 = 8.17, p = 0.043). Kompletan sellarni tip pokazuje jaku, konzistentnu pozitivnu povezanost sa pneumatizacijom prednjeg klinoidnog i pterygoidnog processusa na svim stranama (p ≤ 0.015, često < 0.001). Tip III Vidian kanala je zastupljen u ~ 40%. Vidian kanal Tip I je snažno povezan sa pneumatizacijom pterygoidnih processusa posebno bilateralno (p < 0,001 u svim slučajevima).

Zaključci: Kohorta pokazuje visoko pneumatizovan, hirurški relevantan fenotip sfenoidalnog sinusa, prvenstveno razvojni, a ne simptomatski.

Ključne reči: pneumatizacija sfenoidalnog sinusa, Vidianov kanal, anteriorni klinoidni processus, pterygoidni processus, multidetektorska kompjuterizovana tomografija.

Primljen: 12.02.2026. I **Revidiran:** 07.04.2026. I **Prihvaćen:** 09.04.2026. I **Online First:** 15.04.2026.

Medicinska istraživanja 2026